Cell Reports
Article

Cell PRESS
Open ACCESS

5S Ribosomal RNA Is an Essential Component of a Nascent Ribosomal Precursor Complex that Regulates the Hdm2-p53 Checkpoint

Giulio Donati,[1,2] Suresh Peddigari,[2] Carol A. Mercer,[2] and George Thomas[1,2,*]
[1]Laboratory of Cancer Metabolism, ICO/IDIBELL, Hospital Duran i Reynals, Gran Via de l'Hospitalet, 199-08908 Hospitalet de Llobregat, Barcelona, Spain
[2]Division of Hematology and Oncology, Department of Internal Medicine, College of Medicine, Metabolic Diseases Institute, University of Cincinnati Cancer Center, 3125 Eden Avenue, Cincinnati, OH 45267, USA
*Correspondence: thomasg4@uc.edu
http://dx.doi.org/10.1016/j.celrep.2013.05.045

SUMMARY

Recently, we demonstrated that RPL5 and RPL11 act in a mutually dependent manner to inhibit Hdm2 and stabilize p53 following impaired ribosome biogenesis. Given that RPL5 and RPL11 form a preribosomal complex with noncoding 5S ribosomal RNA (rRNA) and the three have been implicated in the p53 response, we reasoned they may be part of an Hdm2-inhibitory complex. Here, we show that small interfering RNAs directed against 5S rRNA have no effect on total or nascent levels of the noncoding rRNA, though they prevent the reported Hdm4 inhibition of p53. To achieve efficient inhibition of 5S rRNA synthesis, we targeted TFIIIA, a specific RNA polymerase III cofactor, which, like depletion of either RPL5 or RPL11, did not induce p53. Instead, 5S rRNA acts in a dependent manner with RPL5 and RPL11 to inhibit Hdm2 and stabilize p53. Moreover, depletion of any one of the three components abolished the binding of the other two to Hdm2, explaining their common dependence. Finally, we demonstrate that the RPL5/RPL11/5S rRNA preribosomal complex is redirected from assembly into nascent 60S ribosomes to Hdm2 inhibition as a consequence of impaired ribosome biogenesis. Thus, the activation of the Hdm2-inhibitory complex is not a passive but a regulated event, whose potential role in tumor suppression has been recently noted.

INTRODUCTION

The integration of cell growth and cell proliferation is essential for the maintenance of organ size and tissue homeostasis. The rate of cell growth is in large part determined by the rate of protein synthesis and hence the availability of translational machinery, particularly ribosomes. Moreover, misregulation of ribosome biogenesis is associated with extreme forms of aberrant growth, including anemia and cancer (Barna et al., 2008; Ruggero and Pandolfi, 2003; Zhang and Lu, 2009). Ribosomes are composed of a 40S subunit and a 60S subunit, with their biogenesis requiring the coordinate expression of four distinct noncoding ribosomal RNAs (rRNAs) and approximately 80 unique ribosomal proteins (RPs). The 40S subunit is composed of 30 distinct RPs and a single molecule of 18S rRNA, whereas the 60S subunit contains 49 unique RPs and single copies of 28S, 5.8S, and 5S rRNA. Importantly, in contrast to other noncoding rRNAs, which are transcribed in the nucleolus by RNA polymerase I (Pol I), 5S rRNA is transcribed in the nucleus by RNA Pol III.

The importance of ribosome biogenesis in coordinating cell growth and cell division is underscored by the observation that impairment of this process leads to induction of p53 and cell-cycle arrest (Fumagalli and Thomas, 2011; Zhang and Lu, 2009). The critical role of this checkpoint in human pathology was first demonstrated in two hematopoietic disorders, 5q− syndrome and Diamond-Blackfan anemia (DBA) (Draptchinskaia et al., 1999; Gazda et al., 2008), which are characterized by monoallelic deletions or hypomorphic mutations of RP genes. Moreover, patients with these diseases have a high risk of developing myelodysplasia and a wide range of distinct neoplasias later in life, including acute myeloid leukemia, colon carcinoma, and osteogenic sarcoma (Vlachos et al., 2012). The induction of p53 was previously shown to be mediated by the binding and inhibition of human double minute 2 (Hdm2) by a subset of RPs, particularly RPS7, RPL5, RPL11, and RPL23 (Zhang and Lu, 2009). Hdm2 is an E3 ubiquitin ligase, which regulates the proteasome-dependent degradation of p53 and is the main regulator of the tumor suppressor. The complexity of this regulatory circuit is further accentuated by the fact that Hdm2 is a p53 transcriptional target, apparently to ensure p53 downregulation nce an insult has been managed (Barak et al., 1993; Wu et al., 1993).

Previously, we demonstrated that either deletion of RP genes or depletion of their transcripts led to the impairment of ribosome biogenesis and the induction of p53 in a manner dependent on the binding of RPL11 to Hdm2. Moreover, codepletion of

RPL11 was sufficient to suppress the rise in p53 and relieve the cell-cycle block (Fumagalli et al., 2009). Given the role of RPS7, RPL5, and RPL23 in mediating this effect, one may have expected that depleting cells of RPL11 would not have been sufficient to relieve the p53 response. This conundrum led us to the finding that only RPL11 and RPL5, in a mutually dependent manner, are required for p53 induction following disruption of ribosome biogenesis (Fumagalli et al., 2012). Importantly, recent studies demonstrate that this checkpoint may also act as a tumor suppressor in B cell lymphomas overexpressing c-Myc under the control of the immunoglobulin heavy chain promoter and enhancer (Eμ-Myc) (Macias et al., 2010). In part, c-Myc promotes tumorigenesis in this setting by inducing the upregulation of ribosome biogenesis. However, when a cancer-associated single point mutation within the zinc-finger domain of Hdm2, which abolishes its binding to RPL11 and RPL5 but not the alternative reading frame, was knocked into the wild-type locus of the mouse *Mdm2* gene of Eμ-Myc mice, they succumbed much more rapidly to B cell lymphoma than control Eμ-Myc mice (Macias et al., 2010). Thus, this regulatory mechanism appears to constitute a highly sensitive surveillance system to monitor either impairment or hyperactivation of ribosome biogenesis.

In yeast, orthologs of RPL11 and RPL5 form a complex with 5S rRNA prior to their incorporation into the nascent 90S processome, a step mediated by two assembly factors, Rpf2 and Rrs1 (Zhang et al., 2007). It was first shown by Marechal et al. that immune precipitates of Hdm2 contained both RPL5 and 5S rRNA (Marechal et al., 1994). In more recent studies, Horn and Vousden demonstrated that overexpression of either RPL11 or RPL5 alone was sufficient to suppress Hdm2 and induce p53. However, Hdm2 inhibition was more robust when both RPs were coexpressed, an effect mediated by RPL11's ability to recruit RPL5 indirectly to Hdm2 via 5S rRNA (Horn and Vousden, 2008). Together these results led us to predict that in higher eukaryotes, 5S rRNA is part of a complex containing RPL11 and RPL5, which acts to suppress Hdm2 and increase p53, following impairment or hyperactivation of ribosome biogenesis (Fumagalli et al., 2012). However, Li and Gu recently showed that 5S rRNA is required for Hdm4-mediated inhibition of p53 (Li and Gu, 2011). Hdm4 is highly homologous to Hdm2 but is devoid of ligase activity and instead directly binds to p53 to inhibit its transactivation function (Marine and Jochemsen, 2004). Interestingly, the form of 5S rRNA associated with Hdm4 was reported to be the immature form, having two additional uridines at the 3′ terminus (Li and Gu, 2011). This form of 5S rRNA does not interact with RPL5, which only binds the more abundant mature form of 5S rRNA (Steitz et al., 1988; Ciganda and Williams, 2011). This finding raised the possibility that the seemingly contradictory role of 5S rRNA in mediating p53 function may be due to the immature form stabilizing Hdm4, whereas the mature form inhibits Hdm2. The significance of elucidating the molecular mechanisms mediating these two responses is underscored by the importance of p53, Hdm2, and Hdm4, which are misregulated in over 50% of human tumors (Bond et al., 2004; Toledo and Wahl, 2006).

Here, we set out to assess the role of 5S rRNA in mediating p53 stability in cells in which ribosome biogenesis is impaired. We found that directly targeting 5S rRNA with a specific small interfering RNA (siRNA) not only had no effect on total ribosome production (Li and Gu, 2011) but also did not affect nascent 5S rRNA synthesis. We then turned to the potential of depleting cells of TFIIIA, a Pol III cofactor specifically required for 5S rRNA transcription (Engelke et al., 1980; Shastry et al., 1984). Such treatment effectively blocked 5S rRNA biogenesis and 60S subunit production. Inhibition of this process impaired 60S ribosome biogenesis at the same step as depletion of either RPL5 or RPL11. Contrary to earlier findings, all three components are jointly dependent on one another to bind Hdm2 and inhibit p53 degradation in response to impaired ribosome biogenesis. Importantly, we demonstrate that despite the large abundance of the mature RPL5/5S rRNA complex, it is apparently the nascent preribosomal RPL5/RPL11/5S rRNA complex that is redirected from 60S ribosome biogenesis to Hdm2 inhibition upon disruption of ribosome biogenesis and that formation of the complex does not require p53 or Hdm2. The results underscore the importance of a critical regulatory circuit mediated by an apparent nascent RPL5/RPL11/5S rRNA preribosomal complex in controlling p53 levels and cell-cycle progression.

RESULTS

Mature 5S rRNA Binds Both Hdm2 and Hdm4

To examine the role of 5S rRNA on the regulation of p53, we treated U2 OS cells with either a nonsilencing siRNA (si-NS) or one directed against 5S rRNA (si-5S). We found that treatment of U2 OS cells with the si-5S, as compared to those treated with the si-NS, leads to the reduction of Hdm4 protein and the activation of p53-dependent transcription, as judged by the induction of p21 and Hdm2 (Figure 1A), consistent with the findings of Li and Gu (2011). If not a component of the RPL5/RPL11 Hdm2 inhibitory complex, then we would have expected depletion of 5S rRNA to impair 60S ribosome biogenesis and induce p53. It is known that the more abundant mature form of 5S rRNA interacts with Hdm2 (Marechal et al., 1994), whereas it is the immature form that is reported to mediate Hdm4 inhibition of p53 (Li and Gu, 2011). This raised the possibility that the less abundant immature form, potentially the nascent form, is selectively lost by si-5S treatment, leading to the observed activation of p53 (Figure 1A). Unexpectedly, the cloning and sequencing of the 5S rRNA associated with either Hdm4 or Hdm2 (Experimental Procedures) revealed that both represented the 119-residue mature form of 5S rRNA, with no clones representing the larger immature 5S rRNA species (Figure 1B). Thus, the effects of si-5S siRNA treatment on the activation of p53 do not appear to be attributed to the selective loss of the less abundant immature species of 5S rRNA.

Given the findings above, we examined the effect of si-5S treatment on ribosome biogenesis by analyzing total rRNA levels by ethidium bromide (EB) staining and newly synthesized rRNA by pulse labeling with ^{3}H-uridine (Fumagalli et al., 2009). As 5S rRNA is an essential component of the 60S ribosome, suppressing its expression should also affect 28S and 5.8S rRNA processing but not that of 18S rRNA (Dechampesme et al., 1999; Zhang et al., 2007). The EB-stained polyacrylamide gel shows that si-5S depletion, as compared to si-NS, had no effect on total levels of

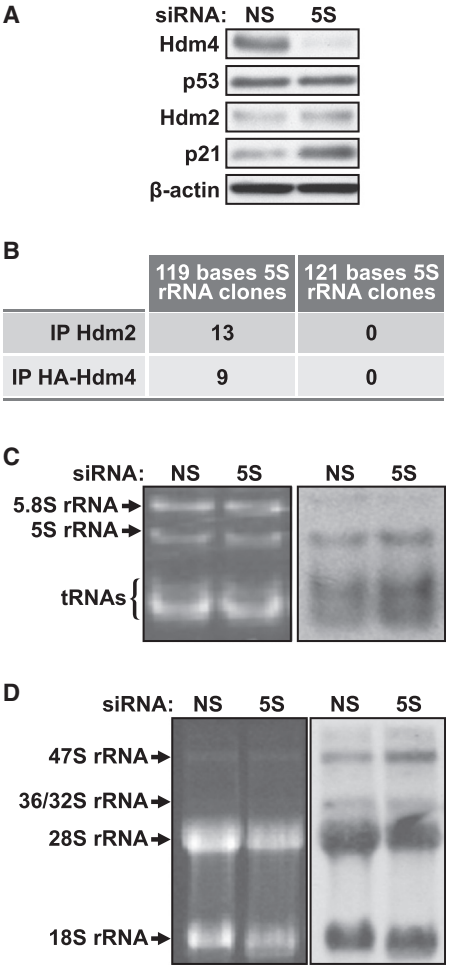

Figure 1. Effect of 5S rRNA-Targeted siRNA on Ribosome Biogenesis

(A) Western blot analysis of expression levels of Hdm4, p53, p21 and Hdm2 and the loading control β-actin in U2 OS cells transfected for 72 hr with si-NS (NS) or si-5S (5S).

(B) 5S rRNA that coimmunoprecipitated with Hdm2 or HA-tagged Hdm4 was cloned and sequenced (Experimental Procedures).

(C) EB-stained TBE-urea polyacrylamide gel (left) and autoradiogram of a northern blot (right) of newly synthesized ^{3}H-uridine-labeled 5S rRNA in U2 OS cells transfected with si-NS or si-5S; 2 μg of total cellular RNA per lane.

(D) EB-stained agarose gel (left) and autoradiogram of a northern blot (right) of total cellular RNA from si-NS or si-5S transfected U2 OS cells labeled with ^{3}H -uridine for 1 hr and then chased for 4 hr in nonlabeled uridine-containing medium; 1 μg of total cellular RNA per lane.

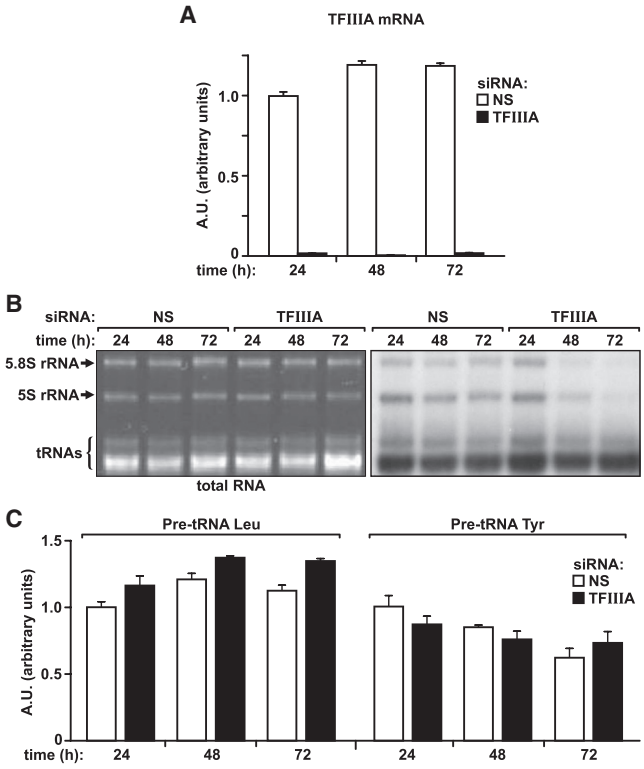

Figure 2. Effect of TFIIIA Depletion on RNA Pol-III-Dependent Transcription

(A) TFIIIA mRNA levels in US OS cells transfected with si-NS or si-TF were evaluated by quantitative real-time PCR. Bar graphs show the mean ±SEM of three samples.

(B) EB-stained TBE-urea polyacrylamide gel (left) and autoradiogram of a northern blot (right) showing newly synthesized ^{3}H-uridine-labeled 5S rRNA in U2 OS cells transfected for 24, 48, and 72 hr with si-NS or si-TF; 2 μg of total cellular RNA per lane.

(C) Quantitative real-time PCR quantification of Leu- and Tyr-tRNA precursors in U2 OS cells transfected as described in (A).

Bar graphs show the mean value ±SEM of three samples. See also Figure S1.

5S rRNA or on 5.8S rRNA (Figure 1C), consistent with the findings of Li and Gu (2011). Moreover, analysis of the larger rRNA species on agarose gels showed no apparent differences in either 28S or 18S rRNA levels (Figure 1D). However, si-5S treatment also had no impact on the incorporation of ^{3}H-uridine into nascent 5S rRNA or into 5.8S and 28S rRNA (Figures 1C and D), which is consistent with the absence of an impaired ribosome biogenesis-induced p53 response, despite the ability of such treatment to repress Hdm4 (Figure 1A) (Li and Gu, 2011). Thus, si-5S treatment leads to loss of Hdm4 and p53 activation but does so independent of impairing 5S rRNA production or nascent ribosome biogenesis.

Depletion of TFIIIA Selectively Impairs 5S rRNA Synthesis

Given the limitations of an siRNA approach in depleting either total or nascent 5S rRNA, we turned to an alternative strategy, depletion of Pol III cofactor TFIIIA/GTF3A, which is specifically required for 5S rRNA transcription. Treatment of U2 OS cells with an siRNA against TFIIIA (si-TF) effectively reduced its messenger RNA (mRNA) levels at each time point examined up to 72 hr posttransfection, as measured by quantitative real-time PCR (Figure 2A). To determine the extent to which si-TF treatment affected mature and nascent pools of 5S rRNA, we followed a similar protocol to that described above (Figures 1C and 1D). As in the case of si-5S treatment, the results of EB staining show that TFIIIA depletion had no observable effect on total levels of 5S rRNA or 5.8S rRNA up to

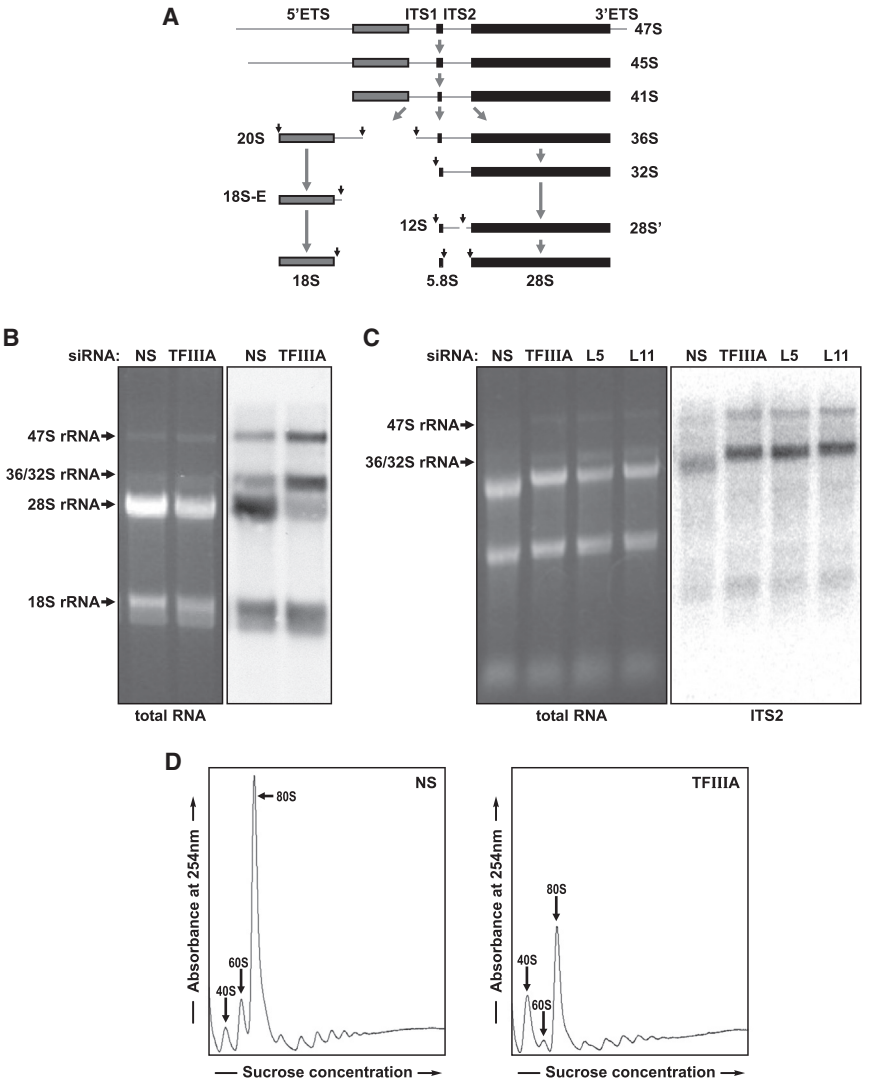

Figure 3. Effect of TFIIIA Depletion on Ribosome Biogenesis

(A) Pre-rRNA processing pathway in mammals.

(B) EB-stained agarose gel (left) and autoradiogram of a northern blot (right) of ^{3}H-uridine-labeled RNA (1 hr pulse and 4 hr chase) from U2 OS cells 72 hr after the transfection of si-NS or si-TF; 1 μg of total cellular RNA per lane.

(C) EB stained agarose gel (left) and northern blot (right) of total RNA extracted from U2 OS cells 72 hr after transfection with siRNAs specific for si-NS (NS), si-TF (TF), RPL5 (L5), or RPL11 (L11). Northern blot hybridized with a probe directed against ITS2 (internal transcribed spacer 2) of precursor rRNA: 1 μg of total cellular RNA per lane.

(D) Polysome profiles of extracts from U2 OS cells transfected with si-NS or si-TF.

72 hr posttransfection (Figure 2B). However, contrary to si-NS- or si-5S-treated cells, those treated with si-TF showed a clear reduction in newly synthesized 5S rRNA, as measured by autoradiography, an effect detected as early as 48 hr posttransfection (Figure 2B). Consistent with 5S rRNA being an essential component of the 60S ribosome, TFIIIA depletion also suppressed nascent 5.8S rRNA production (Figure 2B). That this effect is specific for transcription of 5S rRNA, and no other Pol III transcriptional targets, is shown by the fact that si-TF treatment did not appear to inhibit Pol-III-dependent transcription of total transfer RNA (tRNA) (Figure 2B) or that of leucyl- or tyrosyl-tRNA (Figure 2C). It should be noted that such treatment also led to a reduction in Hdm4 levels (Figure S1), consistent with the requirement of nascent 5S rRNA for its stability. Thus, depletion of TFIIIA does not affect total 5S rRNA levels but effectively suppresses the production of nascent 5S rRNA.

Depletion of TFIIIA Impairs Ribosome Processing

In yeast, mutants of 5S rRNA, as with loss of either RPL5 or RPL11, exhibit impaired processing of 27SB pre-rRNA into a mature 25S rRNA and 5.8S rRNA, retarding 60S ribosome production (Dechampesme et al., 1999). Likewise, disruption of the incorporation of the RPL5/RPL11/5S rRNA preformed complex into the 90S processome leads to the accumulation of the same 27SB pre-rRNA (Zhang et al., 2007). The orthologous steps in mammalian rRNA processing are depicted in Figure 3A. To determine the step at which depletion of TFIIIA inhibited human ribosome biogenesis, we examined rRNA processing in si-TF or si-NS-treated cells pulse-labeled for 1 hr with ^{3}H-uridine, followed by a 4 hr chase with unlabeled uridine. The results revealed a reduction in 28S rRNA production and the accumulation of both the 47/45S and 36/32S rRNA precursor but no effect on 18S rRNA production (Figure 3B). To ensure that this rRNA species represented the 36S/32S rRNA precursor and to determine whether depletion of nascent 5S rRNA impaired the same step of rRNA processing as that induced by depletion of human RPL5 or RPL11, northern blots were probed for the internal transcribed spacer 2 (ITS2) sequence, which resides between the mature 5.8S and 28S rRNA sequence in the 47S rRNA precursor (Figure 3A). In all cases, depletion of any of the three 60S components led to the accumulation of the same 36/32S precursor rRNA in U2 OS cells as compared to cells treated with the si-NS (Figure 3C). Taken together, these results demonstrate that depletion of TFIIIA, as well as either RPL5 or RPL11, impairs ribosome biogenesis at a step that is analogous to that in yeast, at which the RPL5/RPL11/5S rRNA complex is assembled into the 90S processome. Consistent with these findings, analysis of polysome profiles demonstrated that depletion of TFIIIA led to a loss of native 60S ribosomes and an increase in native

40S ribosomes (Figure 3D). In addition, the reduction in the amount of 60S ribosomal subunits relative to the amount of 40S ribosomal subunits led to the increased formation of 43S preinitiation complexes, visualized as half-mer polyribosomes, observed as a pronounced shoulder on the right side of the 80S monosome and polysomal peaks (Figure 3D). We have recently reported similar results for the depletion of RPL5 and RPL11 (Fumagalli et al., 2012), consistent with depletion of TFIIIA affecting the same step of 60S ribosome biogenesis as loss of RPL5 or RPL11.

RPL5, RPL11, and 5S rRNA Are Mutually Dependent on Each Other for p53 Response following Impaired Ribosome Biogenesis

Although depletion of either RPL5 or RPL11 impairs ribosome biogenesis, they are mutually dependent on one another to inhibit Hdm2 and induce p53 (Fumagalli et al., 2012). To determine whether depletion of nascent 5S rRNA exerts a similar response or whether instead its depletion leads to the induction of p53, we treated U2 OS cells, as well as HCT116 and A549 cells, with si-NS, si-Polr1a (the catalytic subunit of the Pol I complex), and si-TF alone or si-TF in combination with si-Polr1a. We have previously shown that silencing of Polr1a induced p53 in response to inhibition rRNA transcription (Donati et al., 2011). The results show that in all cases, TFIIIA mRNA levels were reduced by ≥90% of those observed in si-NS-treated cells (Figure 4A). Such treatment had little to no effect on basal levels of p53 or on the two downstream target genes p21 and Hdm2, whereas depletion of TFIIIA completely reversed the effects on all three responses elicited by Polr1a depletion (Figure 4B). Moreover, consistent with the effects observed on p53 and p21, the depletion of Polr1a led to the accumulation of cells in G1, an effect that was relieved by the codepletion of TFIIIA (Figure 4C). To ensure these effects were specific for TFIIIA depletion, we analyzed two additional siRNAs, one that effectively lowered the levels of the cognate transcript to the same level as the original siRNA and one that had little effect (Figure S2A). The data show that only the two that reduced TFIIIA mRNA levels suppressed the induction of p53, Hdm2, and p21 when codepleted with Polr1a (Figure S2B). Moreover, the suppression of the p53 response by codepletion of TFIIIA was not confined to Polr1a, as the same effect was observed by codepletion of TFIIIA with RPS6 or RPL7a, whose individual depletion leads to disruption of 40S and 60S ribosome biogenesis, respectively (Figure S3A). This was also the case for the induction of p53 and p21 by chemotherapeutic agents known to inhibit ribosome biogenesis: actinomycin D (Perry, 1963) and 5-fluorouracil (Wilkinson and Pitot, 1973) (Figure S3B). Finally, the ability of TFIIIA to suppress the induction of p53, as well as p21 and Hdm2, by Polr1a depletion was not further enhanced by codepletion of either RPL5 or RPL11 (Figure 4D). These findings indicate that all three components are mutually dependent on one another for inhibition of Hdm2.

5S rRNA, RPL5, and RPL11 Binding to Hdm2 Is Mutually Dependent

The results above support a model where impairment of ribosome biogenesis leads to the inhibition of Hdm2 and the

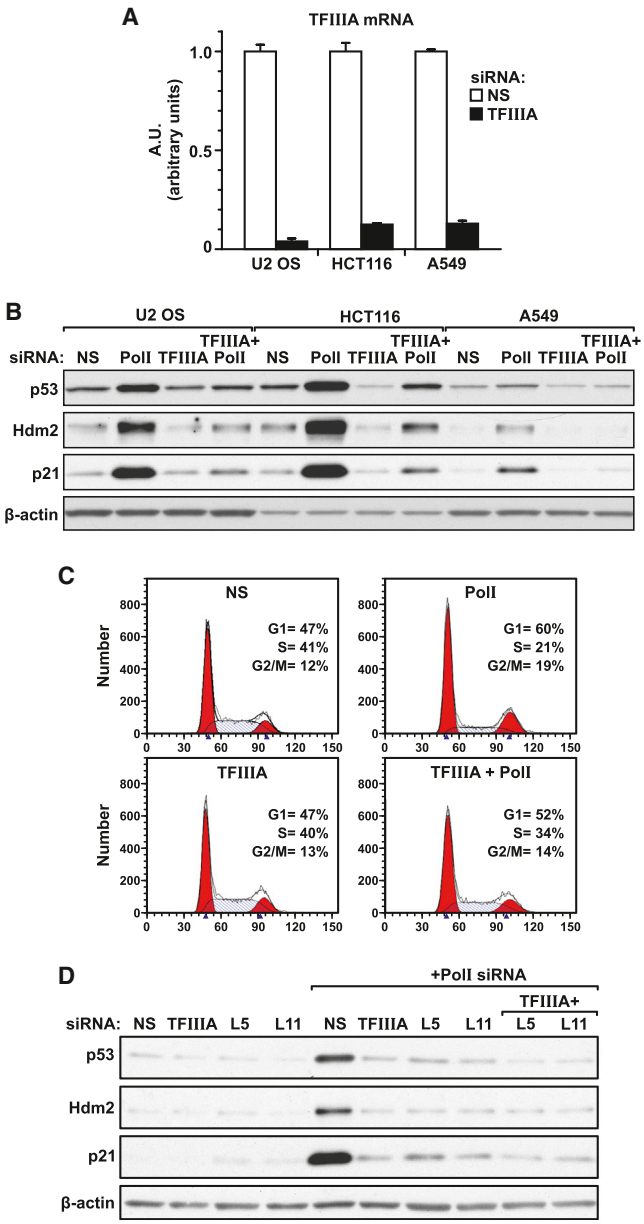

Figure 4. Effect of TFIIIA Depletion on the Stabilization of p53

(A) U2 OS, HCT 116, and A549 cells were transfected for 72 hr with si-NS or si-TF, total RNA was extracted, and TFIIIA mRNA levels were evaluated by quantitative real-time PCR analysis. Bar graphs show the mean ±SEM of three independent experiments.

(B) Western blot analysis showing expression levels of p53, p21, and Hdm2 and the loading control β-actin in U2 OS, A549, and HCT 116 cells 72 hr after transfection with si-NS, si-TF, or an siRNA specific for POLR1A (Pol I).

(C) Cell-cycle phase distribution in U2 OS cells transfected with the indicated siRNAs.

(D) Western blot analyses showing expression levels of p53, p21, and Hdm2 and the loading control β-actin in U2 OS cells transfected for 72 hr with individual or combined siRNAs to NS, TFIIIA, RPL5, RPL11, or Pol I.

See also Figures S2 and S3.

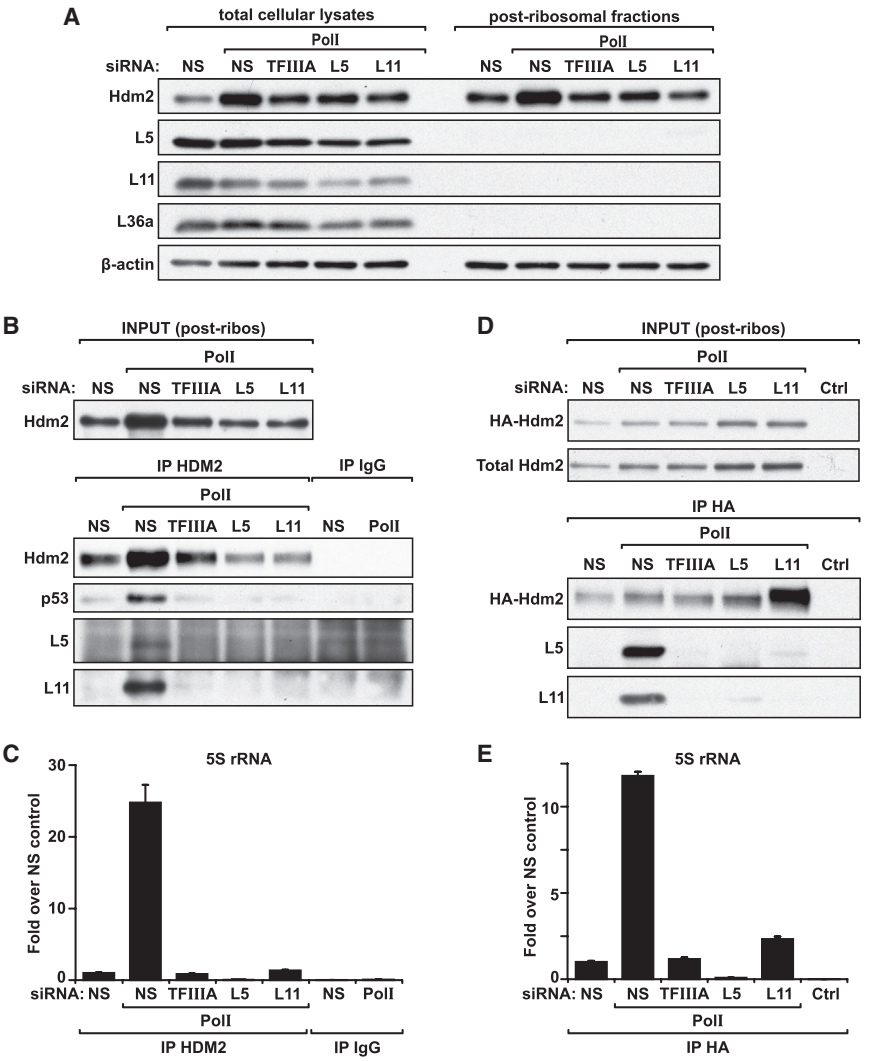

Figure 5. RPL5, RPL11, and 5S rRNA Binding to Hdm2

(A) Western blot analyses showing expression levels of Hdm2, RPL5, RPL11, RPL36a, and β-actin protein from U2 OS cells transfected with control si-NS, si-TF, or siRNAs specific for RPL5 and RPL11 in combination with Pol I siRNA, before (left) and after (right) ultracentrifugation.

(B) U2 OS cells were transfected for 48 hr with either si-NS or Pol I siRNA in combination with siRNA targeted to TFIIIA, RPL5, or RPL11 and then harvested for immunoprecipitation analysis. Western blot analyses show the expression levels of Hdm2 in the postribosomal lysates (INPUT) and of Hdm2, p53, RPL5, and RPL11 immunoprecipitated from cell lysates with anti-Hdm2 rabbit antibody (IP HDM2) or rabbit immunoglobulin G control (IP IgG).

(C) Quantification by quantitative real-time PCR of 5S rRNA associated with Hdm2 or IgG immunoprecipitated complexes, prepared as described in (B). Bar graphs show the mean value ±SEM of three samples.

(D) U2 OS cells were first transfected for 24 hr with si-NS or Pol I siRNA in combination with NS, TFIIA, RPL5, or RPL11 siRNAs and then transfected for an additional 24 hr with an HA-tagged Hdm2 expression plasmid before harvesting for coimmunoprecipitation analysis. Western blot analyses show expression levels of total and exogenous HA-tagged MDM2 in the initial lysates (INPUT) and levels of HA-Hdm2, p53, RPL5, and RPL11 immunoprecipitated with an HA antibody (12CA5) from postribosomal cell lysates. Normal growing, nontransfected U2 OS cells were used as a control (Ctrl).

(E) Quantification by quantitative real-time PCR of 5S rRNA immunoprecipitated with an HA antibody from U2 OS cells transfected as described in (D). Bar graphs show the mean value ±SEM of three samples.

stabilization of p53 in a mutually dependent manner by RPL5, RPL11, and 5S rRNA. As it has been shown that exogenously expressed RPL5 and RPL11 can bind independently to Hdm2 (Bhat et al., 2004; Dai and Lu, 2004; Horn and Vousden, 2007; Lohrum et al., 2003), we reasoned that depletion of any one member should not affect the binding of the others. To test this hypothesis, we immunoprecipitated Hdm2 from cells treated for 48 hr with si-Polr1a alone or together with si-RPL5, si-RPL11, or si-TF and scored for the association of each of the three components with Hdm2. Prior to immunoprecipitation, cell lysates were subjected to high-speed ultracentrifugation to clear mature ribosomes, thus minimizing nonspecific interactions of mature ribosomes during the coimmunoprecipitation (Experimental Procedures). This step does not alter the levels of Hdm2 compared to those of the total lysates, employing β-actin as a control, whereas the majority of ribosomal proteins are cleared from the lysate (Figure 5A). The Hdm2 immunoprecipitates of the postribosomal lysates were then divided in two fractions, which were used for either protein or RNA analysis. Parallel analyses of these immunoprecipitates by western blot or quantitative real-time PCR revealed the presence of RPL5, RPL11, and 5S rRNA (Figures 5B and 5C, respectively). Unexpectedly, depletion of RPL5, RPL11, or TFIIIA abolished the interaction of the other two components with Hdm2 (Figures 5A and 5B), arguing that their binding to Hdm2 is mutually dependent.

Although depletion of RPL5, RPL11, or 5S rRNA abolished the interaction of the other two components with Hdm2, such treatment also reduced the levels of the E3 ligase (Figures 5A and 5B), consistent with Hdm2 being a p53 target. Given the findings of others (Bhat et al., 2004; Dai and Lu, 2004; Horn and Vousden, 2007; Lohrum et al., 2003), this raised the possibility that the reduced amount of Hdm2 recovered by immunoprecipitation may in part explain our inability to detect coimmunoprecipitated RPL5, RPL11, and 5S rRNA. To address this issue, 24 hr following transfection of si-Polr1a alone or together with si-RPL5, si- RPL11, or si-TF, cells were retransfected with a plasmid encoding a hemagglutinin (HA)-tagged Hdm2 (Experimental Procedures). The transcription of Hdm2 from this plasmid

is p53 independent, and the protein is produced in much higher amounts than its endogenous counterpart, which was undetectable in the exposure shown (Figure 5D). After an additional 24 hr, postribosomal lysates were prepared, exogenous HA-Hdm2 was immunoprecipitated, and the interacting proteins and rRNAs were analyzed by western blot or quantitative real-time PCR, respectively. Under these conditions, the expression of HA-tagged Hdm2 was relatively equal as was its immunoprecipitation (Figure 5D). The results show that only in cells treated with si-Polr1a alone were RPL5, RPL11, and 5S rRNA efficiently coimmunoprecipitated with HA-tagged Hdm2 (Figures 5D and 5E, respectively). Thus, the interdependence of endogenous RPL5, RPL11, and 5S rRNA in binding and suppressing Hdm2 appears to be independent of the levels of the E3 ligase.

RPL5, RPL11, and 5S rRNA Are Redirected to Hdm2 following Impaired Ribosome Biogenesis

That the depletion of nascent rRNA, but not total 5S rRNA, was associated with suppressing the induction of p53 following impaired ribosome biogenesis (Figures 2B and 4B) suggests that it is the nascent RPL5/RPL11/5S rRNA precursor complex that is redirected from 60S ribosome biogenesis to the inhibition of Hdm2. In yeast, Rrs1 and Rpf2 are required to load the RPL5/RPL11/5S rRNA precursor complex into the 90S processome (Zhang et al., 2007). The apparent human orthologs of the yeast proteins are hRrs1 and Bxdc1 (Gambe et al., 2009; Hirano et al., 2009). If the nascent RPL5/RPL11/5S rRNA precursor complex is normally loaded onto the 90S processome by hRrs1 and Bxdc1, then one would predict that their depletion would impair ribosome biogenesis at the same stage as loss of RPL5, RPL11, or TFIIIA, but would not be required for Hdm2 inhibition. Consistent with this prediction, depletion of either hRrs1 or Bxdc1 in U2 OS cells, as judged by quantitative real-time PCR of their respective mRNAs (Figure S4), impeded the processing of the 36S/32S rRNA precursor as measured with a probe to ITS2 (Figure 6A), similar to that seen for cells depleted of RPL5, RPL11, or 5S rRNA (Figure 3C), supporting a conserved function for hRrs1 and Bxdc1 in ribosome biogenesis. To determine whether they are implicated in the p53 response induced by impaired ribosome biogenesis, we transfected cells with si-hRrs1 or si-Bxdc1 alone or in combination with si-Polr1a, employing si-TF as a positive control. The results show that, unlike the loss of RPL5, RPL11, or TFIIIA, depletion of either hRrs1 or Bxdc1 led to the induction of p53 and further augmented the response induced by depletion of Polr1a (Figure 6B). This would suggest that hRrs1 or Bxdc1 lie at, or downstream of, the regulatory bifurcation point that mediates the targeting of a RPL5/RPL11/5S rRNA precursor complex to inhibition of Hdm2.

The results above also suggest that binding of such a precursor complex to Hdm2 would be independent of Hdm2 availability, as its overexpression in the absence of impaired ribosome biogenesis does not lead to the recruitment of the RPL5, RPL11, or 5S rRNA (Figures 5D and 5E). To determine whether all three components interact independent of Hdm2, we took advantage of mouse embryo fibroblasts (MEFs) from *Mdm2*$^{-/-}$/*p53*$^{-/-}$-deficient mice (Montes de Oca Luna et al., 1995) treated with a low dose of actinomycin D to impair ribosome biogenesis. Our initial efforts to immunoprecipitate

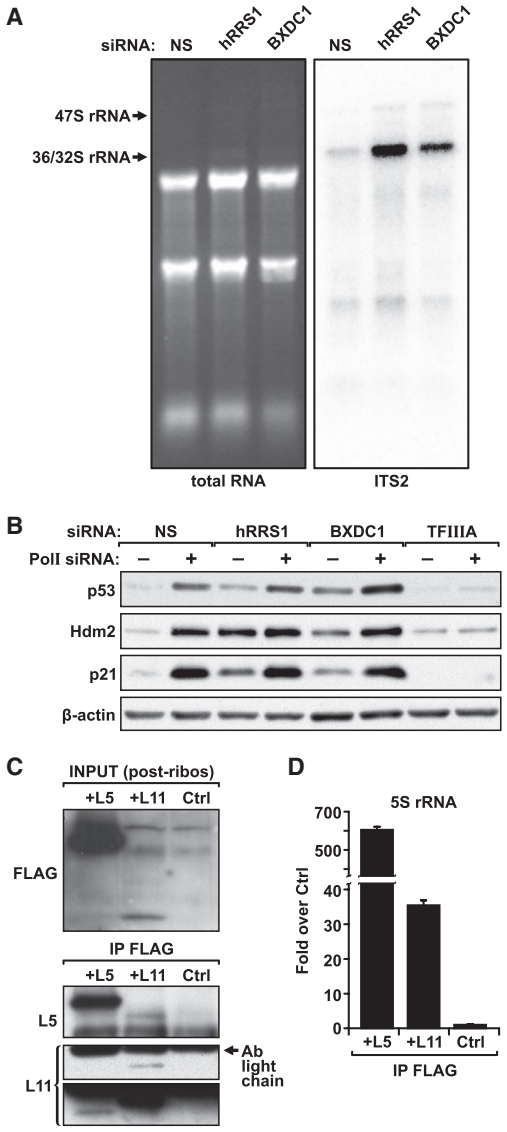

Figure 6. Formation of the RPL5/RPL11/5S rRNA Complex Is Independent of 60S Ribosome Biogenesis and Hdm2

(A) EB-stained agarose gel (left) and northern blot (right) of total RNA extracted from U2 OS cells 72 hr after transfection with NS-, hRRS1-, or BXDC1-specific siRNA. The northern blot was hybridized with a probe directed against ITS2 of precursor rRNA (Figure 3A); 1 μg of total cellular RNA per lane.

(B) Western blot analyses showing expression levels of p53, p21, Hdm2, and the loading control β-actin from U2 OS cells transfected with NS, hRRS1, BXDC1, and TFIIIA siRNAs, alone and in combination with Pol-I-targeted siRNA.

(C) Mdm2/p53 knockout MEFs were transfected for 24 hr with FLAG-tagged RPL5 or RPL11 and treated for 5 hr with 5 ng/ml actinomycin D before harvesting. Postribosomal lysates from control (Ctrl) and FLAG-expressing MEFs were immunoprecipitated with a FLAG antibody. Western blot analyses show FLAG-tagged proteins in the postribosomal lysates (INPUT) and both endogenous and exogenous RPL5 and RPL11 proteins that coimmunoprecipitated with the FLAG antibody. Light and dark exposure times are shown for the RPL11 blot.

(D) Quantification by quantitative real-time PCR of 5S rRNA that immunoprecipitated with FLAG antibody from the postribosomal fraction of *MDM2/p53* knockout MEFs transfected and treated as described in (C).

See also Figure S4.

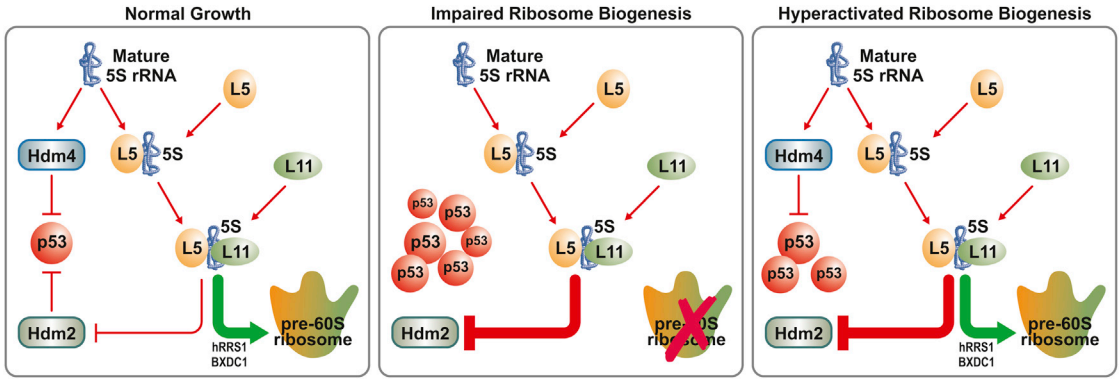

Figure 7. Model of p53 Regulation
See text for explanation.

endogenous RPL5 and RPL11 after high-speed centrifugation to remove mature ribosomes failed (data not shown), potentially due to low levels of the endogenous RPL5/RPL11/5S rRNA complex. Therefore, we ectopically expressed FLAG-tagged RPL5 or RPL11 in *Mdm2*$^{-/-}$/*p53*$^{-/-}$ MEFs as reporters. Despite the fact that we expressed a great deal more of FLAG-tagged RPL5 than FLAG-tagged RPL11 (Figure 6C, top), we clearly detect endogenous RPL5 in a coimmunoprecipitation (coIP) with the exogenous FLAG-RPL11 and endogenous RPL11 in a coIP with the FLAG-RPL5 (Figure 6C, bottom). Moreover, these signals were absent in untransfected control cells (Figure 6C). In parallel, as compared to untransfected *Mdm2*$^{-/-}$/*p53*$^{-/-}$ MEFs, we found a 610-fold and a 35-fold enrichment of 5S rRNA associated with FLAG-RPL5 and FLAG-RPL11, respectively (Figure 6D). The 20-fold enrichment in 5S rRNA observed in association with FLAG-RPL5, compared to the FLAG-RPL11, may reflect its higher expression and the ability of RPL5 and 5S rRNA to form an abundant complex independent of the 60S ribosome (Steitz et al., 1988). These results support the model that RPL5, RPL11, and 5S rRNA form a complex independent of Hdm2. Taken together, these findings suggest that upon impairment of ribosome biogenesis, the nascent RPL5/RPL11/5S rRNA precursor complex is redirected to Hdm2 rather than into nascent 60S ribosomes (Figure 7).

DISCUSSION

We recently demonstrated that the role of many RPs, including RPS7 and RPL23, previously implicated in the inhibition of Hdm2 and the induction of p53, may potentially be attributed to a general global inhibition of protein synthesis rather than specific inhibition of Hdm2 (Fumagalli et al., 2012). The exceptions appear to be RPL5 and RPL11, which are mutually dependent on one another to elicit this response (Fumagalli et al., 2012), a finding recently substantiated by others (Bursać et al., 2012). Moreover, RPL5 and RPL11 have been implicated in a c-Myc-induced Hdm2-dependent tumor suppressor checkpoint (Macias et al., 2010). Our results suggest a central role for 5S rRNA in this complex. Indeed, given the earlier findings that implicated 5S rRNA as an RPL5/RPL11 interacting partner in regulating Hdm2 (Horn and Vousden, 2008; Marechal et al., 1994), we reasoned that 5S rRNA would also be required to induce p53 following impairment of ribosome biogenesis (Fumagalli et al., 2012). Although this appears to be the case, the recent studies presented by Li and Gu and those carried out here demonstrate that 5S rRNA is also a positive regulator of Hdm4 (Li and Gu, 2011). Interestingly, 5S rRNA levels are not affected by siRNA treatment (Li and Gu, 2011; Figure 1), raising the possibility that si-5S rRNA may act by disrupting the interaction of Hdm4 with a specific 5S rRNA subpopulation. Moreover, in contrast to Li and Gu, our results would argue that this effect, like that of impaired ribosome biogenesis, is mediated predominantly by the mature form of 5S rRNA (Figure 1B).

Disruption of ribosome biogenesis leads to rapid degradation of Hdm4 by Hdm2, releasing the block on p53, as does the binding of an apparent RPL5/RPL11/5S rRNA complex to Hdm2, the two steps leading to the concerted activation of p53 (Li and Gu, 2011). The role of 5S rRNA in mediating Hdm4 inhibition of p53 would be an attractive alternative mechanism to link rates of ribosome biogenesis to cell-cycle progression. However, 5S rRNA exists in an abundant extraribosomal population (Knight and Darnell, 1967), with levels reported to be twice those of the other noncoding rRNAs (Gottlieb and Steitz, 1989), suggesting it may not be a sensitive sensor. Instead, this role appears to reside in the RPL5/RPL11/5S rRNA complex, which may be consumed in exponentially growing cells into nascent 60S ribosomes, leading to a potential coordinate decrease in p53 levels (Donati et al., 2011). As cells become confluent, p53 levels most likely rise in an RPL5/RPL11/5S rRNA-complex-dependent manner (Bhat et al., 2004). Given that levels of RPL5 in the nucleolus, like 5S rRNA, are in excess compared to all other RPs (Phillips and McConkey, 1976) might suggest that the rate-limiting step would be RPL11 availability; however, ectopic expression of RPL11 without coexpression of RPL5 was not as robust in inhibiting Hdm2 as expression of the two RPs together (Horn and Vousden, 2008). Our findings suggest that it is more likely that the inhibitory step is a regulated event leading to redirection of a nascent RPL5/RPL11/5S rRNA complex from the 60S ribosome to Hdm2 (Figure 7). It will be important to discern in future studies whether the Hdm4/5S rRNA complex is a target

of the Hdm2/RPL5/RPL11/5S rRNA complex under impaired ribosome biogenesis or whether it has a more complex role in a feedback regulatory circuit that is mediated by the state of nascent ribosome biogenesis.

Recent studies have also implied a critical role for RPL11 in independently controlling the levels of p53 through inhibition of Hdm2 (Sasaki et al., 2011). Here, the protein interacting with carboxyl terminus 1 (PICT1) of the tumor suppressor PTEN has been implicated as a negative regulator of RPL11 (Sasaki et al., 2011). Sasaki and coworkers demonstrated that colorectal and esophageal tumors, which are p53 wild-type and express low levels of PICT1, have a significantly better prognosis (Sasaki et al., 2011). Moreover, they demonstrated that inducible deletion of the floxed PICT1 gene in MEFs led to induction of p53 and apoptosis. They show this effect was mediated by the release of RPL11, a PICT1 binding protein, from the nucleolus to the nucleoplasm, where it can bind and inhibit Hdm2. Consistent with these findings, they observed that siRNA depletion of RPL11 suppressed p53 that was induced by loss of PICT1. However, in contrast with our findings on impaired ribosome biogenesis (Fumagalli et al., 2012), they found these effects were independent of RPL5 (Sasaki et al., 2011). This finding is consistent with the failure of RPL5 to be released from the nucleolus following depletion of PICT1. We find that PICT1 shares a significant degree of homology with the yeast 60S processing enzyme Nop53 (Thomson and Tollervey, 2005), and in preliminary studies its depletion appears to selectively impede nascent 60S ribosomal biogenesis (A. Gentilella, G.D., and G.T., unpublished data). Thus, we would have predicted that the induction of p53 by loss of PICT1 would have been dependent on the RPL5/RPL11/5S rRNA complex. It will be of interest to determine the relationship of PICT1 with RPL5, RPL11, and 5S rRNA and the mechanism through which they interact with one another to regulate Hdm2.

Earlier, we demonstrated that regulation of 40S and 60S ribosome biogenesis led to the induction of p53 by an RPL5- and RPL11-dependent mechanism (Fumagalli et al., 2009, 2012). However, in the case of impaired 40S ribosome biogenesis, this led to the translational upregulation of 5′ terminal oligopyrimidine tract (TOP) mRNAs, including RPL11 (Fumagalli et al., 2009). Initially, we reasoned this effect was triggered by the continued synthesis of 60S ribosomes and the resulting consumption of nascent RPL11 into 60S ribosomal subunits (Fumagalli et al., 2009). However, we recently found that codepletion of both a 60S and 40S ribosomal protein, a condition where competition for RPL11 would be eliminated, still led to the translational upregulation of RPL11 mRNA (Fumagalli et al., 2012). These findings argue that although the two mechanisms exploited the same molecular components to inhibit Hdm2, they were differentially regulated. Moreover, both responses were insulated from one another, as the impairment of both subunits led to an additive effect on p53 induction and a more severe cell-cycle arrest (Fumagalli et al., 2012). The questions that arise from these studies are: what is sensed as damage in each case and what are the mechanisms by which these responses lead to the induction of p53? It was initially argued to be a passive response associated with disruption of the nucleolus, based largely from studies employing actinomycin D (Rubbi and Milner, 2003). However, this does not seem to be the case; instead, it appears that activation of p53 is associated with the disruption of nascent ribosome biogenesis (Fumagalli et al., 2009). Interestingly, the studies presented here suggest that it is the nascent RPL5/RPL11/5S rRNA complex that elicits this response, consistent with the recent findings of Bursać et al. implicating newly synthesized RPL5 and RPL11 in this response (Bursać et al., 2012). At this stage, it will be important to isolate the presumed RPL5/RPL11/5S rRNA complex induced by impaired 60S and 40S ribosome biogenesis to determine whether there are differences in their molecular makeup. Likewise, the mechanisms involved in upregulation of 5′TOP translation should shed insight into the underlying mechanisms that signal the execution of the response to impaired ribosome biogenesis.

The pathological consequences of insufficient RPs were first recognized in DBA and 5q− syndrome, diseases characterized by severe macrocytic anemia and bone marrow failure (Fumagalli and Thomas, 2011). In mouse models of 5q− syndrome and DBA, the anemic phenotype can be largely reversed by depletion of p53 (Jones et al., 2008). Studies in mice further demonstrate that not all ribosome protein insufficiencies present with equivalent phenotypes. For example, heterozygous deletion of RPS6 caused embryonic lethality that was delayed, but not rescued, by loss of p53 (Panić et al., 2006), which is consistent with the fact that mutations in RPS6 have not been reported in DBA patients. Even so, conditional depletion of RPS6 in juvenile or adult mice leads to a very similar DBA phenotype (McGowan et al., 2011), which is rescued by loss of p53. Thus, the lesion in ribosome biogenesis is not the apparent cause of the disease but rather activation of p53 (Fumagalli and Thomas, 2011). This raises questions regarding the role of a RPL5/RPL11/5S rRNA complex in DBA and 5q− syndrome, as hypomorphic mutations in RPL5 and RPL11 have been identified in DBA (Gazda et al., 2008). Interestingly, the congenital phenotypes caused by mutations in RPL5 and RPL11 are generally more severe than those observed with other RP gene mutations (Gazda et al., 2008). In developing better therapeutic approaches, it will be critical to determine whether the RPL5/RPL11/5S rRNA complex is implicated in this response or whether instead p53 stabilization is mediated by a distinct mechanism.

DBA as well as 5q− syndrome patients have an increased risk of developing cancer, including acute myeloid leukemia, with a cumulative incidence of 20% by the age of 46 (Vlachos et al., 2012). This is consistent with findings in both *Drosophila* and zebrafish that hypomorphic alleles of RP genes act as haploid-insufficient tumor suppressors (Amsterdam et al., 2004; Stewart and Denell, 1993). In zebrafish, 11 of the 12 lines developed malignant peripheral nerve sheath tumors (MPNST), each heterozygous for a distinct RP mutation (Amsterdam et al., 2004). Interestingly, in each case, the zebrafish with hypomorphic mutation of an RP gene that also developed MPNSTs displayed reduced levels of p53 (MacInnes et al., 2008). Questions that arise from this observation are, do cancers of DBA and 5q− syndrome patients result from reduced p53 levels? If so, what is the underlying mechanism that allows such tumors to become aggressive if translational capacity is impaired? One of the mechanisms attributed to p53's role as a tumor suppressor is through repression of the transcription of the

proto-oncogene c-Myc, through either direct transcriptional repression (Ho et al., 2005) or induction of miR145 (Sachdeva et al., 2009). It has been known for some time that a primary function of c-Myc is the transcriptional upregulation of ribosomal components mediated through all three RNA polymerases (van Riggelen et al., 2010). Thus, in a tumor setting, a hypomorphic allele of an RP gene may not be limiting if c-Myc is hyperactivated and the other allele is intact. Interestingly, recent studies suggest that p53 suppresses c-Myc-driven tumors through an RPL5/RPL11 checkpoint (Bywater et al., 2012; Macias et al., 2010) and that RPL11 can suppress the expression of c-Myc through a negative feedback loop that controls c-Myc mRNA stability (Challagundla et al., 2011; Dai et al., 2007). It will be of clinical relevance to determine whether these effects are independently regulated by RPL11, RPL5, and 5S rRNA or by an RPL5/RPL11/5S rRNA complex.

EXPERIMENTAL PROCEDURES

Cell Culture, Transfections, and Drug Treatments

U2 OS cells and *p53/MDM2* double-knockout (DKO) MEFs were cultured and maintained as previously described (Fumagalli et al., 2009). Lipofectamine RNAiMAX (Invitrogen) and Opti-MEM medium (Invitrogen) were used according to the manufacturer's protocol for siRNA transfections. The siRNA sequences for 5S rRNA, RPL5, and RPL11 have been previously described (Fumagalli et al., 2009, 2012; Li and Gu, 2011); siRNA sequences for *GTF3A*, *POLR1A*, *hRRS1*, and *BXDC1* are listed in Table S1. Nonsilencing siRNA (QIAGEN) was used as a control and for normalization. Plasmids encoding HA-Hdm4, HA-Hdm2, FLAG-L11, and FLAG-L5 have been previously described (Dai et al., 2007; Dai and Lu, 2004). MEFs were transfected with plasmids using the Amaxa Nucleofector (Lonza) 24 hr before harvest. Actinomycin D (BioVision Technologies) was used at a final concentration of 5 ng/ml.

RNA Extraction, Reverse Transcription, Real-Time PCR, and Northern Blot

Cells were harvested and total RNA was extracted with TRI Reagent (Molecular Research Center) according to the manufacturer's instructions. Whole-cell RNA was reverse transcribed using the Superscript III kit (Invitrogen). Real-time PCR was performed on an ABI 7900HT (Applied Biosystems) using the 2-ΔΔCT method for analysis (Livak and Schmittgen, 2001). The mean ΔCT value of the control sample was used in each experiment to calculate the ΔΔCT value of sample replicates. Primer sequences used for SYBR green real-time PCR analysis of β-actin, 5S rRNA, pre-tRNAs, RPL11, and RPL5 have been previously described (Fumagalli et al., 2009, 2012; Livak and Schmittgen, 2001; Shor et al., 2010; Winter et al., 2000) Other primers (listed in Table S2) were designed using the IDT PrimerQuest online tool (http://eu.idtdna.com/SCITOOLS/Applications/PrimerQuest/Default.aspx). Northern blot analysis was performed as previously described (Fumagalli et al., 2009) with a probe specific for human ITS2 (Table S2).

Autoradiographic Analysis of rRNA Processing and 5S rRNA Synthesis

To evaluate rRNA processing, newly synthesized RNA was labeled by incubating the cells for 45 min in medium containing 1.2 μCi [5,6-^{3}H]-uridine (Perkin Elmer) per ml. Pulsed-labeled cells were then washed into medium containing 1 mM nonradioactive uridine (Sigma) and incubated for 4 hr at 37°C in 5% CO_2. Following extraction, 1 μg of total RNA was size-separated by electrophoresis on a 1% agarose-formaldehyde gel. To evaluate 5S rRNA synthesis, total RNA was extracted following the 2 hr pulse and 2 μg of each RNA sample was electrophoresed on a TBE-urea 10% polyacrylamide gel. Following electrophoresis, the RNA in both cases was transferred to Hybond N+ membrane (Amersham Biosciences) and the blots were sprayed with En3Hancer (Perkin Elmer) and exposed to Kodak BioMax MS film (Kodak) at −80°C for autoradiography.

Total Cellular Proteins Extraction and Western Blot Analysis

Total protein extraction and SDS-PAGE were performed as previously described (Fumagalli et al., 2009). Briefly, cells were lysed on ice in extraction buffer (50 mM Tris-HCl [pH 8], 250 mM NaCl, 1% Triton X-100, 0.25% sodium deoxycholate, 0.05% SDS, 1 mM dithiothreitol [DTT], and protease inhibitors cocktail [Roche]). The lysates were cleared by centrifugation and quantified by Bradford protein assay (Bio-Rad). Primary antibodies for western blotting were as follows: mouse monoclonal anti-FLAG (M2; Sigma-Aldrich), anti-p21 (SX118; BD Pharmingen), anti-Hdm2 (SMP14; Santa Cruz Biotechnology), anti-p53 (BP53-12; Sigma-Aldrich), anti-rpL11 (3A4A7; Invitrogen), anti-rpL36a (43-A; Santa Cruz), rabbit polyclonal anti-p53 (FL393; Santa Cruz), anti-Hdm4 (Bethyl Laboratories), anti-β-actin (Sigma-Aldrich), and anti-rpL5 (a gift from H. Lu and M.S. Dai).

Immunoprecipitation

For immunoprecipitation, cells were lysed on ice in immunoprecipitation buffer (25 mM Tris HCl [pH 7.5], 150 mM KCl, 5 mM $MgCl_2$, 1 mM EGTA, 1mM DTT, 10% glycerol, 0.8% Igepal/NP40, and protease inhibitors cocktail [Roche]). The lysates were cleared by centrifugation and quantified by Bradford protein assay (Bio-Rad). Ribosomes were pelleted by ultracentrifugation (200,000 × *g* for 2 hr at 4°C) to obtain postribosomal supernatants. Equivalent amounts of protein (~1 mg for each sample) were incubated at 4°C with rotation overnight in immunoprecipitation buffer with anti-MDM2 (H-221; Santa Cruz), anti-HA (12CA5; prepared from a hybridoma), or anti-FLAG (M2; Sigma-Aldrich). Protein A- or G-coated agarose beads (Santa Cruz) were added to the extracts and mixed by rotation for an additional 2 hr at 4°C. The beads were washed four times with immunoprecipitation buffer, with each sample being divided into two aliquots before the fourth wash. Following final centrifugation, one aliquot was resuspended in protein loading buffer for western blot analysis; the other aliquot was resuspended in TRI reagent (Molecular Research Center) to recover immunoprecipitated RNA for 5S rRNA real time PCR analysis, as described above.

Polysome Profiles and Cell-Cycle Analysis

Preparation of extracts for polysome profiles and sucrose gradient analysis were as described previously (Fumagalli et al., 2009), except that gradients were analyzed on a Gradient Station (Biocomp Instruments) equipped with an EM-1 Econo UV monitor (Bio-Rad). Cell-cycle analyses were performed as described previously (Fumagalli et al., 2009).

SUPPLEMENTAL INFORMATION

Supplemental Information includes four figures and two tables and can be found with this article online at http://dx.doi.org/10.1016/j.celrep.2013.05.045.

ACKNOWLEDGMENTS

We are indebted to H. Lu, M.S. Dai, G. Lozano, S. Volarevic, and J. Chen for providing critical materials for these studies. We thank P. Hexley for the cytofluorimetric assays and are thankful to G. Doerman for his expertise in preparing the figures. We would also like to acknowledge T. Teng and S. Kozma for critiquing the manuscript. This study was supported by a fellowship from the Vanini-Cavagnino legacy (to G.D.). G.T. is supported by grants from the Spanish Ministry of Science and Innovation (SAF2011-24967), the Instituto de Salud Carlos III (ISIS) (IIS10/00015/P), the CIG European Commission (PCIG10-GA-2011-304160), the NIH/NIDDK (1RC1-DK087680), and the NCI/NIH (R01CA158768).

Received: March 27, 2013
Revised: May 8, 2013
Accepted: May 31, 2013
Published: July 3, 2013

REFERENCES

Amsterdam, A., Sadler, K.C., Lai, K., Farrington, S., Bronson, R.T., Lees, J.A., and Hopkins, N. (2004). Many ribosomal protein genes are cancer genes in zebrafish. PLoS Biol. *2*, E139.

Barak, Y., Juven, T., Haffner, R., and Oren, M. (1993). mdm2 expression is induced by wild type p53 activity. EMBO J. *12*, 461–468.

Barna, M., Pusic, A., Zollo, O., Costa, M., Kondrashov, N., Rego, E., Rao, P.H., and Ruggero, D. (2008). Suppression of Myc oncogenic activity by ribosomal protein haploinsufficiency. Nature *456*, 971–975.

Bhat, K.P., Itahana, K., Jin, A., and Zhang, Y. (2004). Essential role of ribosomal protein L11 in mediating growth inhibition-induced p53 activation. EMBO J. *23*, 2402–2412.

Bond, G.L., Hu, W., Bond, E.E., Robins, H., Lutzker, S.G., Arva, N.C., Bargonetti, J., Bartel, F., Taubert, H., Wuerl, P., et al. (2004). A single nucleotide polymorphism in the MDM2 promoter attenuates the p53 tumor suppressor pathway and accelerates tumor formation in humans. Cell *119*, 591–602.

Bursać, S., Brdovčak, M.C., Pfannkuchen, M., Orsolić, I., Golomb, L., Zhu, Y., Katz, C., Daftuar, L., Grabušić, K., Vukelić, I., et al. (2012). Mutual protection of ribosomal proteins L5 and L11 from degradation is essential for p53 activation upon ribosomal biogenesis stress. Proc. Natl. Acad. Sci. USA *109*, 20467–20472.

Bywater, M.J., Poortinga, G., Sanij, E., Hein, N., Peck, A., Cullinane, C., Wall, M., Cluse, L., Drygin, D., Anderes, K., et al. (2012). Inhibition of RNA polymerase I as a therapeutic strategy to promote cancer-specific activation of p53. Cancer Cell *22*, 51–65.

Challagundla, K.B., Sun, X.X., Zhang, X., DeVine, T., Zhang, Q., Sears, R.C., and Dai, M.S. (2011). Ribosomal protein L11 recruits miR-24/miRISC to repress c-Myc expression in response to ribosomal stress. Mol. Cell. Biol. *31*, 4007–4021.

Ciganda, M., and Williams, N. (2011). Eukaryotic 5S rRNA biogenesis. Wiley Interdiscip. Rev. RNA *2*, 523–533.

Dai, M.S., and Lu, H. (2004). Inhibition of MDM2-mediated p53 ubiquitination and degradation by ribosomal protein L5. J. Biol. Chem. *279*, 44475–44482.

Dai, M.S., Arnold, H., Sun, X.X., Sears, R., and Lu, H. (2007). Inhibition of c-Myc activity by ribosomal protein L11. EMBO J. *26*, 3332–3345.

Dechampesme, A.M., Koroleva, O., Leger-Silvestre, I., Gas, N., and Camier, S. (1999). Assembly of 5S ribosomal RNA is required at a specific step of the pre-rRNA processing pathway. J. Cell Biol. *145*, 1369–1380.

Donati, G., Bertoni, S., Brighenti, E., Vici, M., Treré, D., Volarevic, S., Montanaro, L., and Derenzini, M. (2011). The balance between rRNA and ribosomal protein synthesis up- and downregulates the tumour suppressor p53 in mammalian cells. Oncogene *30*, 3274–3288.

Draptchinskaia, N., Gustavsson, P., Andersson, B., Pettersson, M., Willig, T.N., Dianzani, I., Ball, S., Tchernia, G., Klar, J., Matsson, H., et al. (1999). The gene encoding ribosomal protein S19 is mutated in Diamond-Blackfan anaemia. Nat. Genet. *21*, 169–175.

Engelke, D.R., Ng, S.Y., Shastry, B.S., and Roeder, R.G. (1980). Specific interaction of a purified transcription factor with an internal control region of 5S RNA genes. Cell *19*, 717–728.

Fumagalli, S., and Thomas, G. (2011). The role of p53 in ribosomopathies. Semin. Hematol. *48*, 97–105.

Fumagalli, S., Di Cara, A., Neb-Gulati, A., Natt, F., Schwemberger, S., Hall, J., Babcock, G.F., Bernardi, R., Pandolfi, P.P., and Thomas, G. (2009). Absence of nucleolar disruption after impairment of 40S ribosome biogenesis reveals an rpL11-translation-dependent mechanism of p53 induction. Nat. Cell Biol. *11*, 501–508.

Fumagalli, S., Ivanenkov, V.V., Teng, T., and Thomas, G. (2012). Suprainduction of p53 by disruption of 40S and 60S ribosome biogenesis leads to the activation of a novel G2/M checkpoint. Genes Dev. *26*, 1028–1040.

Gambe, A.E., Matsunaga, S., Takata, H., Ono-Maniwa, R., Baba, A., Uchiyama, S., and Fukui, K. (2009). A nucleolar protein RRS1 contributes to chromosome congression. FEBS Lett. *583*, 1951–1956.

Gazda, H.T., Sheen, M.R., Vlachos, A., Choesmel, V., O'Donohue, M.F., Schneider, H., Darras, N., Hasman, C., Sieff, C.A., Newburger, P.E., et al. (2008). Ribosomal protein L5 and L11 mutations are associated with cleft palate and abnormal thumbs in Diamond-Blackfan anemia patients. Am. J. Hum. Genet. *83*, 769–780.

Gottlieb, E., and Steitz, J.A. (1989). Function of the mammalian La protein: evidence for its action in transcription termination by RNA polymerase III. EMBO J. *8*, 851–861.

Hirano, Y., Ishii, K., Kumeta, M., Furukawa, K., Takeyasu, K., and Horigome, T. (2009). Proteomic and targeted analytical identification of BXDC1 and EBNA1BP2 as dynamic scaffold proteins in the nucleolus. Genes Cells *14*, 155–166.

Ho, J.S., Ma, W., Mao, D.Y., and Benchimol, S. (2005). p53-Dependent transcriptional repression of c-myc is required for G1 cell cycle arrest. Mol. Cell. Biol. *25*, 7423–7431.

Horn, H.F., and Vousden, K.H. (2007). Coping with stress: multiple ways to activate p53. Oncogene *26*, 1306–1316.

Horn, H.F., and Vousden, K.H. (2008). Cooperation between the ribosomal proteins L5 and L11 in the p53 pathway. Oncogene *27*, 5774–5784.

Jones, N.C., Lynn, M.L., Gaudenz, K., Sakai, D., Aoto, K., Rey, J.P., Glynn, E.F., Ellington, L., Du, C., Dixon, J., et al. (2008). Prevention of the neurocristopathy Treacher Collins syndrome through inhibition of p53 function. Nat. Med. *14*, 125–133.

Knight, E., Jr., and Darnell, J.E. (1967). Distribution of 5 s RNA in HeLa cells. J. Mol. Biol. *28*, 491–502.

Li, M., and Gu, W. (2011). A critical role for noncoding 5S rRNA in regulating Mdmx stability. Mol. Cell *43*, 1023–1032.

Livak, K.J., and Schmittgen, T.D. (2001). Analysis of relative gene expression data using real-time quantitative PCR and the 2(-Delta Delta C(T)) method. Methods *25*, 402–408.

Lohrum, M.A., Ludwig, R.L., Kubbutat, M.H., Hanlon, M., and Vousden, K.H. (2003). Regulation of HDM2 activity by the ribosomal protein L11. Cancer Cell *3*, 577–587.

Macias, E., Jin, A., Deisenroth, C., Bhat, K., Mao, H., Lindström, M.S., and Zhang, Y. (2010). An ARF-independent c-MYC-activated tumor suppression pathway mediated by ribosomal protein-Mdm2 Interaction. Cancer Cell *18*, 231–243.

MacInnes, A.W., Amsterdam, A., Whittaker, C.A., Hopkins, N., and Lees, J.A. (2008). Loss of p53 synthesis in zebrafish tumors with ribosomal protein gene mutations. Proc. Natl. Acad. Sci. USA *105*, 10408–10413.

Marechal, V., Elenbaas, B., Piette, J., Nicolas, J.C., and Levine, A.J. (1994). The ribosomal L5 protein is associated with mdm-2 and mdm-2-p53 complexes. Mol. Cell. Biol. *14*, 7414–7420.

Marine, J.C., and Jochemsen, A.G. (2004). Mdmx and Mdm2: brothers in arms? Cell Cycle *3*, 900–904.

McGowan, K.A., Pang, W.W., Bhardwaj, R., Perez, M.G., Pluvinage, J.V., Glader, B.E., Malek, R., Mendrysa, S.M., Weissman, I.L., Park, C.Y., and Barsh, G.S. (2011). Reduced ribosomal protein gene dosage and p53 activation in low-risk myelodysplastic syndrome. Blood *118*, 3622–3633.

Montes de Oca Luna, R., Wagner, D.S., and Lozano, G. (1995). Rescue of early embryonic lethality in mdm2-deficient mice by deletion of p53. Nature *378*, 203–206.

Panić, L., Tamarut, S., Sticker-Jantscheff, M., Barkić, M., Solter, D., Uzelac, M., Grabusić, K., and Volarević, S. (2006). Ribosomal protein S6 gene haploinsufficiency is associated with activation of a p53-dependent checkpoint during gastrulation. Mol. Cell. Biol. *26*, 8880–8891.

Perry, R.P. (1963). Selective effects of actinomycin D on the intracellular distribution of RNA synthesis in tissue culture cells. Exp. Cell Res. *29*, 400–406.

Phillips, W.F., and McConkey, E.H. (1976). Relative stoichiometry in ribosomal proteins in HeLa cell nucleoli. J. Biol. Chem. *251*, 2876–2881.

Rubbi, C.P., and Milner, J. (2003). Disruption of the nucleolus mediates stabilization of p53 in response to DNA damage and other stresses. EMBO J. *22*, 6068–6077.

Ruggero, D., and Pandolfi, P.P. (2003). Does the ribosome translate cancer? Nat. Rev. Cancer *3*, 179–192.

Sachdeva, M., Zhu, S., Wu, F., Wu, H., Walia, V., Kumar, S., Elble, R., Watabe, K., and Mo, Y.Y. (2009). p53 represses c-Myc through induction of the tumor suppressor miR-145. Proc. Natl. Acad. Sci. USA *106*, 3207–3212.

Sasaki, M., Kawahara, K., Nishio, M., Mimori, K., Kogo, R., Hamada, K., Itoh, B., Wang, J., Komatsu, Y., Yang, Y.R., et al. (2011). Regulation of the MDM2-P53 pathway and tumor growth by PICT1 via nucleolar RPL11. Nat. Med. *17*, 944–951.

Shastry, B.S., Honda, B.M., and Roeder, R.G. (1984). Altered levels of a 5 S gene-specific transcription factor (TFIIIA) during oogenesis and embryonic development of Xenopus laevis. J. Biol. Chem. *259*, 11373–11382.

Shor, B., Wu, J., Shakey, Q., Toral-Barza, L., Shi, C., Follettie, M., and Yu, K. (2010). Requirement of the mTOR kinase for the regulation of Maf1 phosphorylation and control of RNA polymerase III-dependent transcription in cancer cells. J. Biol. Chem. *285*, 15380–15392.

Steitz, J.A., Berg, C., Hendrick, J.P., La Branche-Chabot, H., Metspalu, A., Rinke, J., and Yario, T. (1988). A 5S rRNA/L5 complex is a precursor to ribosome assembly in mammalian cells. J. Cell Biol. *106*, 545–556.

Stewart, M.J., and Denell, R. (1993). Mutations in the *Drosophila* gene encoding ribosomal protein S6 cause tissue overgrowth. Mol. Cell. Biol. *13*, 2524–2535.

Thomson, E., and Tollervey, D. (2005). Nop53p is required for late 60S ribosome subunit maturation and nuclear export in yeast. RNA *11*, 1215–1224.

Toledo, F., and Wahl, G.M. (2006). Regulating the p53 pathway: in vitro hypotheses, in vivo veritas. Nat. Rev. Cancer *6*, 909–923.

van Riggelen, J., Yetil, A., and Felsher, D.W. (2010). MYC as a regulator of ribosome biogenesis and protein synthesis. Nat. Rev. Cancer *10*, 301–309.

Vlachos, A., Rosenberg, P.S., Atsidaftos, E., Alter, B.P., and Lipton, J.M. (2012). Incidence of neoplasia in Diamond Blackfan anemia: a report from the Diamond Blackfan Anemia Registry. Blood *119*, 3815–3819.

Wilkinson, D.S., and Pitot, H.C. (1973). Inhibition of ribosomal ribonucleic acid maturation in Novikoff hepatoma cells by 5-fluorouracil and 5-fluorouridine. J. Biol. Chem. *248*, 63–68.

Winter, A.G., Sourvinos, G., Allison, S.J., Tosh, K., Scott, P.H., Spandidos, D.A., and White, R.J. (2000). RNA polymerase III transcription factor TFIIIC2 is overexpressed in ovarian tumors. Proc. Natl. Acad. Sci. USA *97*, 12619–12624.

Wu, X., Bayle, J.H., Olson, D., and Levine, A.J. (1993). The p53-mdm-2 autoregulatory feedback loop. Genes Dev. *7*(7A), 1126–1132.

Zhang, J., Harnpicharnchai, P., Jakovljevic, J., Tang, L., Guo, Y., Oeffinger, M., Rout, M.P., Hiley, S.L., Hughes, T., and Woolford, J.L., Jr. (2007). Assembly factors Rpf2 and Rrs1 recruit 5S rRNA and ribosomal proteins rpL5 and rpL11 into nascent ribosomes. Genes Dev. *21*, 2580–2592.

Zhang, Y., and Lu, H. (2009). Signaling to p53: ribosomal proteins find their way. Cancer Cell *16*, 369–377.

Cell PRESS
Open ACCESS

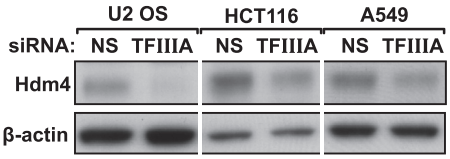

Figure S1. Hdm4 Expression Is Reduced in Cells Depleted of TFIIIA, Related to Figure 2

Western blot analysis showing expression levels of Hdm4 and the loading control β-actin in U2 OS, A549 and HCT116 cells 72 hr after transfection with siRNA specific for TFIIIA.

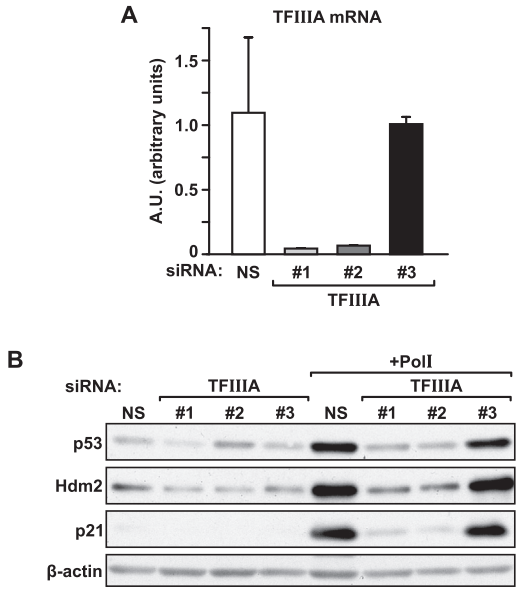

Figure S2. Specificity of TFIIIA Depletion-Mediated Inhibition of p53 Stabilization by Impaired Ribosome Production, Related to Figure 4

(A) U2 OS cells were transfected for 48 hr with 3 different siRNAs targeting TFIIIA expression, total RNA was extracted, and TFIIIA mRNA levels were evaluated by quantitative real-time PCR analysis. Bar graphs show the mean values, ± s.e.m., of three independent experiments. siRNA #1 was used in experiments shown throughout the paper.

(B) Western blot analysis showing expression levels of p53, p21, Hdm2 and β- actin in U2 OS cells transfected for 72 hr with 3 different siRNAs specific for TFIIIA, individually and in combination with PolI siRNA.

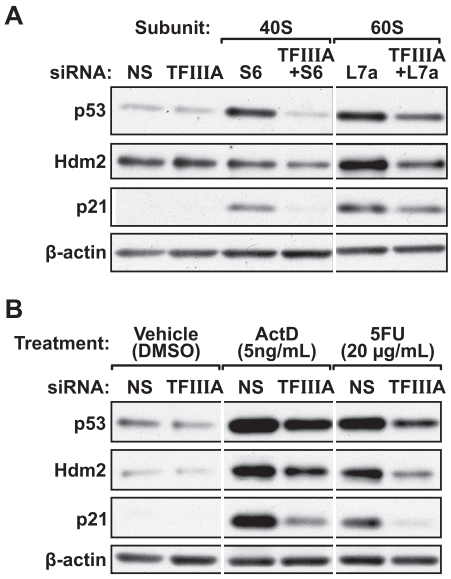

Figure S3. TFIIIA Depletion Inhibits p53 Activation in Response to Specific Forms of Ribosome Biogenesis Impairment, Related to Figure 4

(A) Western blot analyses showing expression levels of p53, p21, Hdm2 and β-actin in U2 OS cells transfected for 48 hr with NS, TFII IA, RPS6 and RPL7a siRNA, individually and in combination as depicted.

(B) Western blot analyses showing expression levels of p53, p21, Hdm2 and β-actin in U2 OS cells transfected for 72 hr with NS or TFIIIA siRNA, and treated for 16 hr with vehicle (DMSO), 5 ng/ml Actinomycin D(ActD) or 20 ug/ml 5-Fluorouracil (5FU).

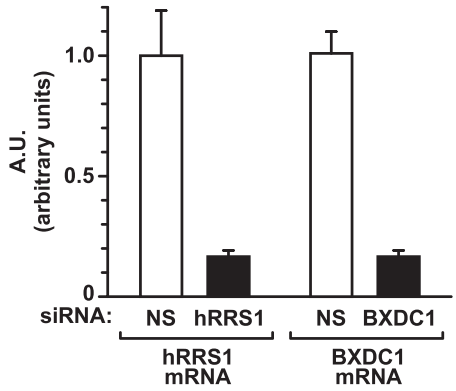

Figure S4. Quantitative Real-Time PCR Analysis Showing siRNA-Mediated Depletion of hRRS1 and BXDC1 mRNA Expression, Related to Figure 6

U2 OS cells were transfected for 72 hr with siRNA specific for hRRS1 or BXDC1. Transcript levels of hRRS1 and BXDC1 were evaluated by quantitative real-time PCR analysis.